PCCP

Covalent Crosslinking in Gas-Phase Biomolecular Ions. An Account and Perspective

Journal:	*Physical Chemistry Chemical Physics*
Manuscript ID	CP-PER-10-2023-004879.R1
Article Type:	Perspective
Date Submitted by the Author:	31-Oct-2023
Complete List of Authors:	Turecek, Frantisek; University of Washington - Seattle Campus, Department of Chemistry

SCHOLARONE™
Manuscripts

Covalent Crosslinking in Gas-Phase Biomolecular Ions. An Account and Perspective

František Tureček

Department of Chemistry, Bagley Hall, Box 351700, University of Washington, WA 98195-1700, USA

Photochemical crosslinking in gas-phase ion complexes has been introduced as a method to study biomolecular structures and dynamics. Emphasis has been on carbene-based crosslinking induced by photodissociation of diazirine-tagged ions. The features that characterize gas-phase crosslinking include (1) complex formation in electrospray droplets that allows for library-type screening; (2) well defined stoichiometry of the complexes due to mass-selective isolation; (3) facile reaction monitoring and yield determination, and (4) post-crosslinking structure analysis by tandem mass spectrometry that has been combined with hydrogen-deuterium exchange, UV-vis action spectroscopy, and ion mobility measurements. In this account, examples are given of peptide-peptide, peptide-nucleotide, and peptide-ligand crosslinking that chiefly used carbene-based reactions. The pros and cons of gas-phase crosslinking are discussed. Nitrile-imine based crosslinking in gas-phase ions is introduced as a promising new approach to ion structure analysis that offers high efficiency and has the potential for wide ranging applications.

Introduction

Crosslinking typically refers to the formation of covalent bonds between components of non-covalent complexes or different parts within the same biomolecule. Among the variety of crosslinking strategies,[1] the one of particular interest here concerns reactive intermediates produced transiently by photodissociation of stable functional groups (Scheme 1).
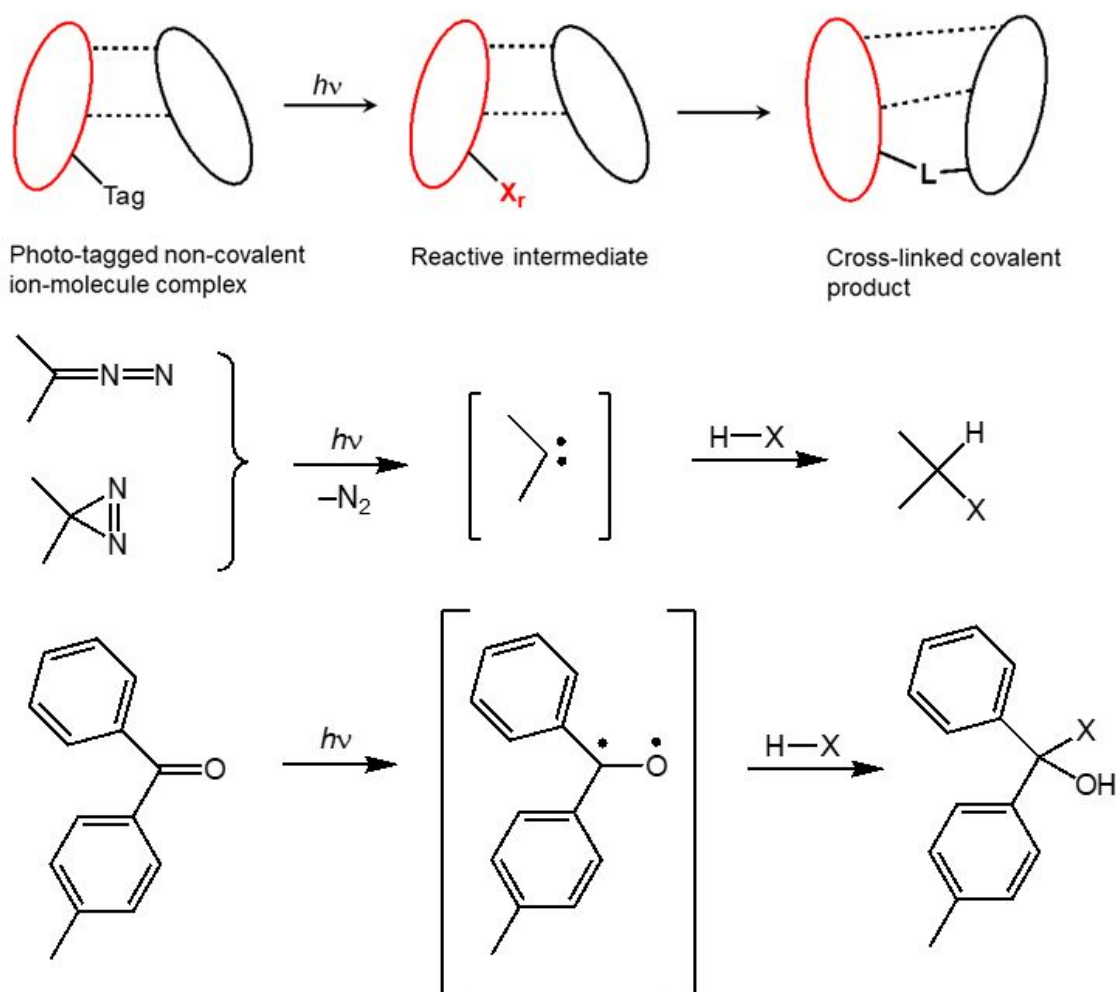
Scheme 1. Photochemical crosslinking.

The functional group is introduced as a tag into one of the components where upon photodissociation it produces a transient intermediate (X_r) that reacts spontaneously by forming a covalent bond at a sterically accessible position. The detected bond formation is used to assign point-to-point distance constraints that can provide information on the spatial arrangement of the reacting regions in the biomolecule or non-covalent complex. Crosslinking differs from other well-established high-resolution methods of structure analysis, such as X-ray crystallography, NMR

spectroscopy, and cryo-electron microscopy that can provide, at various levels of accuracy, atomic coordinates, and thus represent absolute, *de novo* methods. In contrast to these, crosslinking is considered a low-resolution method that can provide information that is complementary to that obtainable by other low-resolution methods, such as Förster resonance energy transfer,[2,3] ion mobility mass spectrometry,[4] and small-angle X-ray scattering.[5] In addition to their low resolution, these methods often require preliminary knowledge of some critical aspects of molecular structure, e.g., protein α-helix or β-sheet, which are often inferred from high resolution data. Thus, crosslinking and other low-resolution methods are rarely, if at all, used for *de novo* structure determination.

The concept of crosslinking and photoaffinity labeling has been introduced by Westheimer *et al*.[6] and Knowles and coworkers,[7] in the 1960s. The reactive intermediates that have been employed include nitrenes[8] and carbenes[9,10] produced by photodissociation, as well as the triplet states formed by photoexcitation in benzophenone-tagged proteins.[11-14] Stable carbene sources, such as diazirines[15-17] and diazoalkanes[18] have been used extensively in photoaffinity labeling and foot printing studies of various biomolecules.[10,19-21] The reactive carbene is generated by photodissociation (e.g., at 350-360 nm from diazirines) and reacts rapidly with various bonds in the target molecule. Addition to the double bond[22] and insertion into C–H bonds[23,24] have been studied in detail for simple carbenes and hydrocarbon targets. The products have been identified by spectroscopic analysis,[25,26] such as EPR spectroscopy,[27] and the reaction kinetics has been studied by laser flash photolysis,[28] analysis of kinetic isotope effects,[29] and quantum mechanical tunneling.[29] The insertion reactions have been found to have very low activation energies.[24-26] In parallel, carbene insertion reactions have been used to achieve covalent crosslinking in non-covalent complexes that almost always involved polar compounds, such as peptides, proteins, etc.[1,10] where low activation energies were presumed to facilitate covalent bond formation.

Compared with other methods using chemical reagents, the principal advantage of photochemical crosslinking is that, in contrast to X-ray and NMR, it does not require purified substrates, and can be carried out in a variety of environments such as lipid bilayers and living cells.[30-34] Crosslinking of proteins has been greatly enabled by the introduction of tagged amino acids that can be recognized by the cellular machinery and incorporated into expressed proteins. Amino acids that are labeled in the side chain with the diazirine group, such as photoleucine, photomethionine,[35] photoproline, and photolysine[36] (Figure 1), are recognized by the transfer

3

RNAs for the corresponding standard amino acids and can be incorporated into expressed proteins to be used for carbene-based photo crosslinking.[37] An excellent recent review of crosslinking in solution combined with mass spectrometry analysis has been published by Sinz and coworkers.[1]
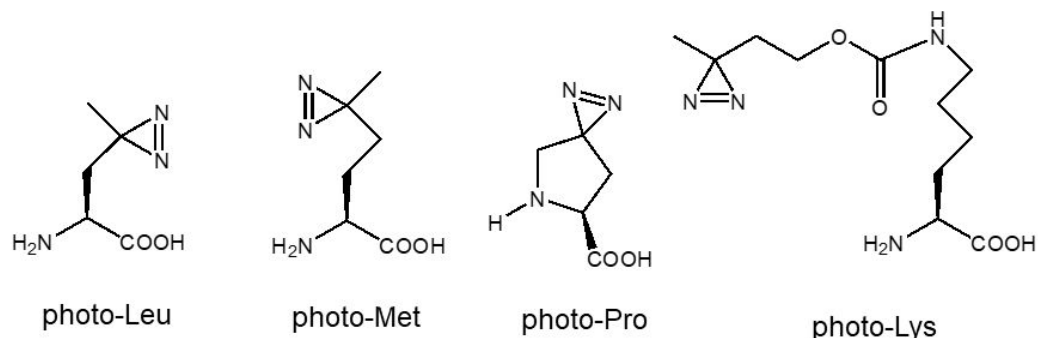

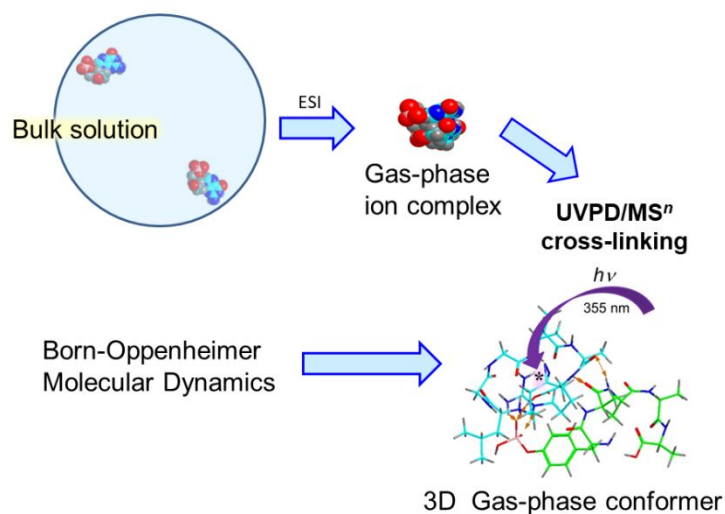photo-Leu   photo-Met   photo-Pro   photo-Lys

Figure 1. Diazirine-tagged amino acids available commercially. The diazirine labeled residues are denoted with an asterisk (L*, M*, P*, K*, etc.) in the text.

Gas-Phase Crosslinking with Transient Carbenes: General Features. The universal nature of carbene crosslinking has spawned the idea of using this technique in a *de novo* approach to elucidate structures of non-covalent complexes of gas-phase biomolecular ions.[38] The workflow for steps involved in gas-phase crosslinking is shown in Figure 2. The components in an approximately 1:1 stoichiometric ratio are electrosprayed from bulk solution to microdroplets, achieving a substantial concentration increase that favors the formation of complexes which are transferred to the gas phase as ions.

Figure 2. Workflow of the experimental and computational approach to gas-phase crosslinking.

In this way, even weak complexes that could not be analyzed by solution spectroscopic methods can be obtained as gas-phase ions and analyzed by tandem mass spectrometry. The complex ion produced by electrospray ionization (ESI) is selected by its mass-to-charge ratio (*m/z*) and probed by photodissociation tandem mass spectrometry. Laser irradiation generates the reactive group (X_r) that can undergo crosslinking to the target counterpart. The experiments are accompanied by

theoretical calculations, starting with Born-Oppenheimer molecular dynamics (BOMD) to generate and sort out protonation isomers and conformers (Scheme 2).
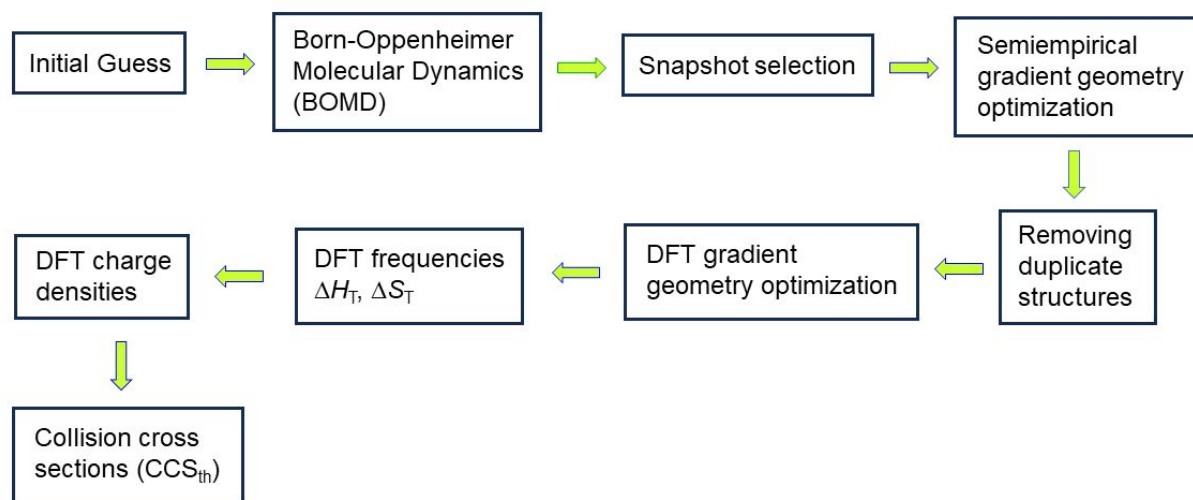

Scheme 2. Workflow of computational analysis.

We have been using enhanced semiempirical methods such as PM6-D3H4 that captures hydrogen bonds and dispersion interactions in the complexes,[39] and running BOMD on the high-level Cuby4 platform developed by Řezáč.[40] In the next step along this computational process, multiple selected complex structures are fully optimized by density functional theory (DFT) methods and ranked by their relative Gibbs energies. The optimized structures and atomic charge densities can be further used for calculations of collision cross sections (CCS), which are structurally relevant parameters obtainable by ion mobility measurements.[41] The experimental localization of crosslinked regions and CCS data along with computational structure and energy analysis represent a powerful approach that allows one to achieve *de novo* structure assignments for ion complexes.

It should be noted that the above-mentioned carbene-based crosslinking is fundamentally different from other reactions forming covalent bonds in gas-phase ions, such as non-selective photodissociation of small peptide complexes at 157 nm,[42] or gas-phase anion-cation reactions of active esters with peptide *N*-terminus.[43,44] Non-selective photoexcitation at 157 nm does not target a particular functional group and thus cannot be used for structure analysis of the complex. Ion-ion reactions do not address non-covalent complexes whereas the interaction between the gas-phase reagents is dominated by strong ion-ion attractive interactions.
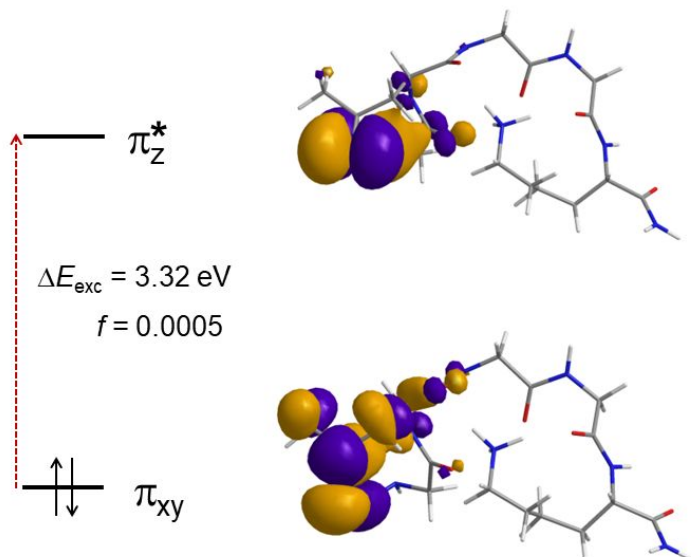
Gas-phase crosslinking shares some features with solution methods in that it does not require laborious sample preparation and thus is suitable for fast screening of complex formation.

However, it has some specific features that distinguish it from analogous reactions in the condensed phase. First, the tagged compounds are converted into gas-phase ions by a suitable soft ionization method, such as ESI, which raises the question of the stability of the precursor diazirine group. ESI of diazirine-tagged peptides has been shown to preserve the diazirine ring without decomposition or isomerization, so singly and multiply charged diazirine-tagged peptide cations can be generated, selected by mass, and subjected to photodissociation.[45-48]   Second, photodissociation changes the mass of the ion, so that the reaction progress is readily monitored, and the 1:1 carbene-target stoichiometry is well defined. Third, the diazirine chemistry in tagged peptide ions has been studied and shown to involve proton- and electron-catalyzed reactions that were specific for gas-phase ions. For example, collision-induced dissociation of the photo-leucine containing peptide amide ions, $(GL*GG-NH_2 + H)^+$ and $(GL*GGK-NH_2 + H)^+$, has been found to involve loss of N_2 from the diazirine ring in competition with standard peptide
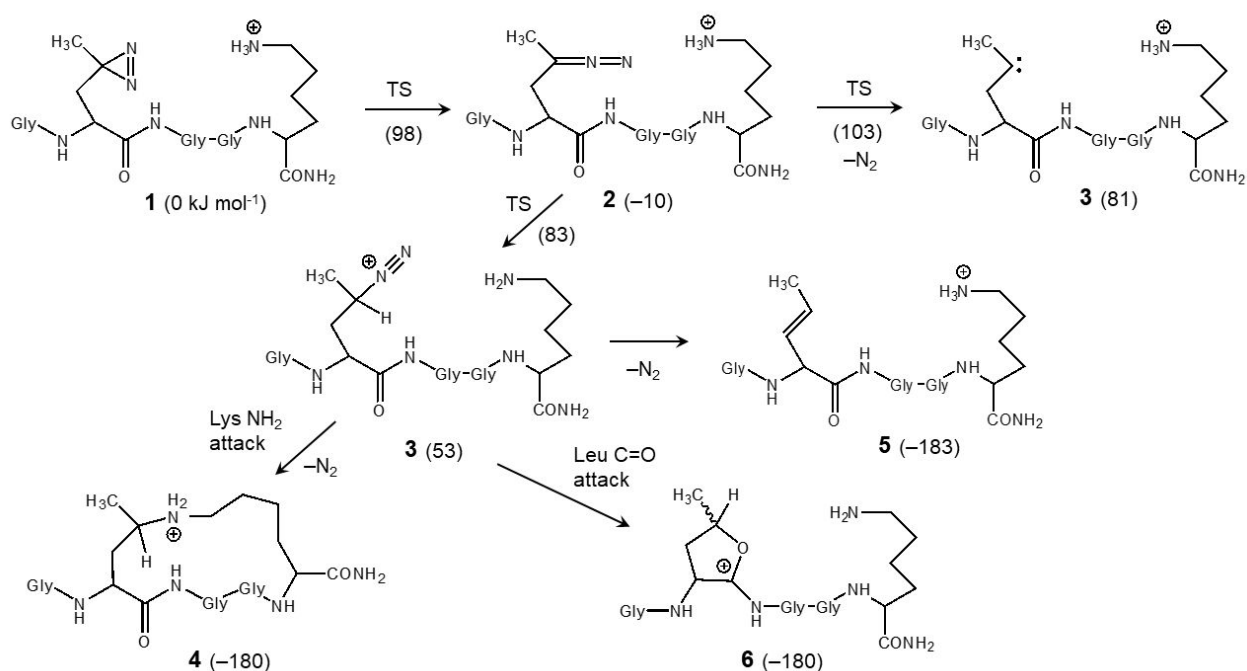
Scheme 3. Isomerizations and dissociations of $(GL*GGK-NH_2 + H)^+$. The relative energies in kJ mol^{-1} are from M06-2X/6-311++G(2d,p) calculations and include zero-point vibrational energy corrections.[45]

backbone cleavages.[45] The reaction mechanism has been studied with the help of deuterium labeling, and the energetics of the competing reactions has been established by density functional theory (DFT) calculations (Scheme 3). These studies have revealed that isomerization of the transient carbene (**3**) to an alkene (**5**) is a highly exothermic reaction, e.g., $\Delta H_{g,0}$ (**3** →**5**)= –264 kJ mol^{-1} in Scheme 3, which is typical of carbene-alkene isomerizations. This feature is particularly relevant for gas-phase ions where collisional energy dissipation to the surrounding rarefied gas is slow.[49,50] Photodissociation of diazirine and its derivatives[10,15] is usually carried out at 355 nm, targeting the weak $\pi_{xy} \rightarrow \pi_z*$ transition to the first excited singlet state (Figure 3).

π_z^*

$\Delta E_{exc} = 3.32$ eV

$f = 0.0005$

π_{xy}

Figure 3. Molecular orbitals in the ground and excited state of (GL*GGK-NH$_2$ + H)$^+$ ion. The excitation energy (ΔE_{exc}) and oscillator strength (f) are from M06-2X/6-311++G(2d,p) time-dependent DFT calculations.

The 355 nm wavelength is conveniently provided as the third harmonics of an Nd-YAG laser. The photon energy (3.49 eV, 337 kJ mol^{-1}) is more than sufficient for not only breaking the diazirine ring (**1** → **2** in Scheme 3), but also for expelling N$_2$ from the diazoalkane intermediate **2** to form carbene **3**. In contrast to photolysis in the condensed phase where the diazoalkane intermediate can be trapped by cooling, irradiation in the gas phase does not result in the formation of stable diazoalkane intermediates. This has been established by infrared multiphoton dissociation (IRMPD) action spectroscopy and UV photodissociation of diazirine-tagged peptide fragment ions that were generated by highly exothermic electron-transfer dissociation.[51] In that study, IRMPD has found no bands at 2100 cm^{-1} which would be characteristic of the diazoalkane C=N=N group. UV photodissociation at 355 nm resulted in loss of N$_2$ which was off-resonance with the calculated absorption of the C=N=N diazoalkane group to the first and second excited states at 530 and 252 nm, respectively (Figure 4).[51]
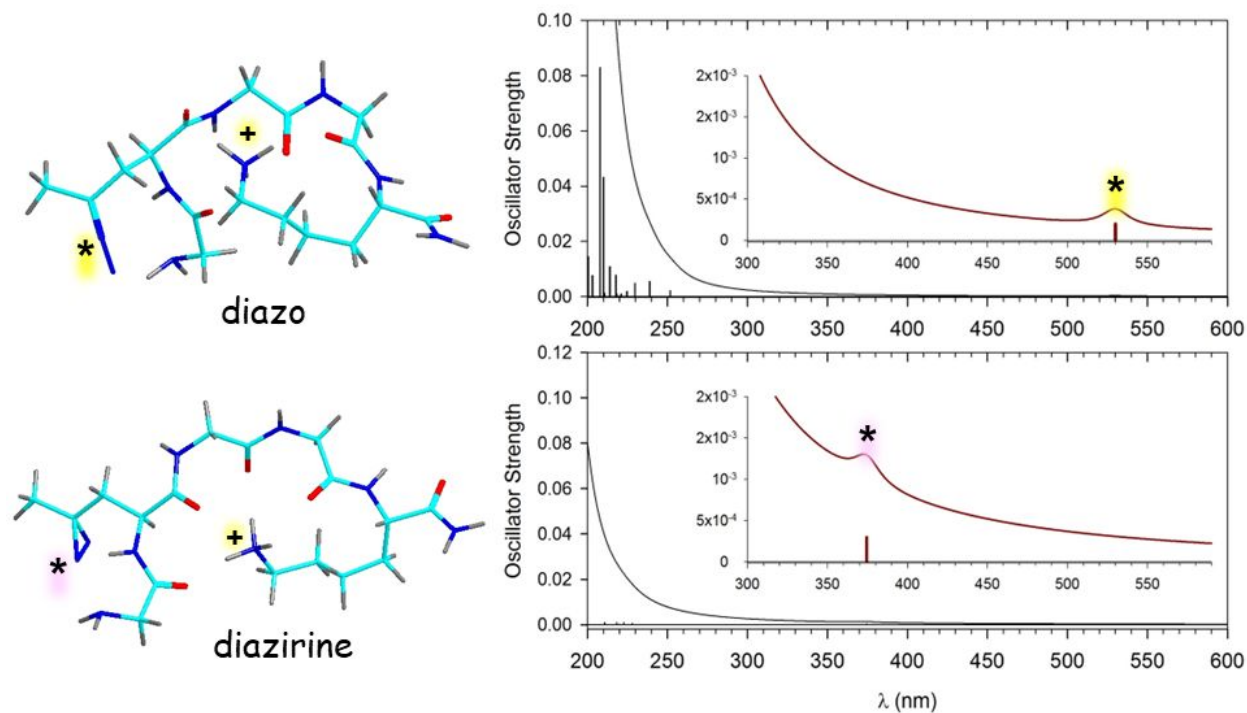
Figure 4.   M06-2X/6-31+G(d,p) optimized structures and calculated absorption spectra of (GL*GGK-NH$_2$ + H)$^+$ with the diazo (**2,** top) and diazirine (**1,** bottom) groups.

Another specific feature of carbene chemistry in the gas phase is the absence of reactions with solvent. In a protic solvent, the very high carbene basicity[52,53] favors the formation of a contact pair between the solvent molecule and a carbocation formed by protonation of the transient carbene.[54-59] The contact pair has a short half-life and can collapse to form a C–O bond in the
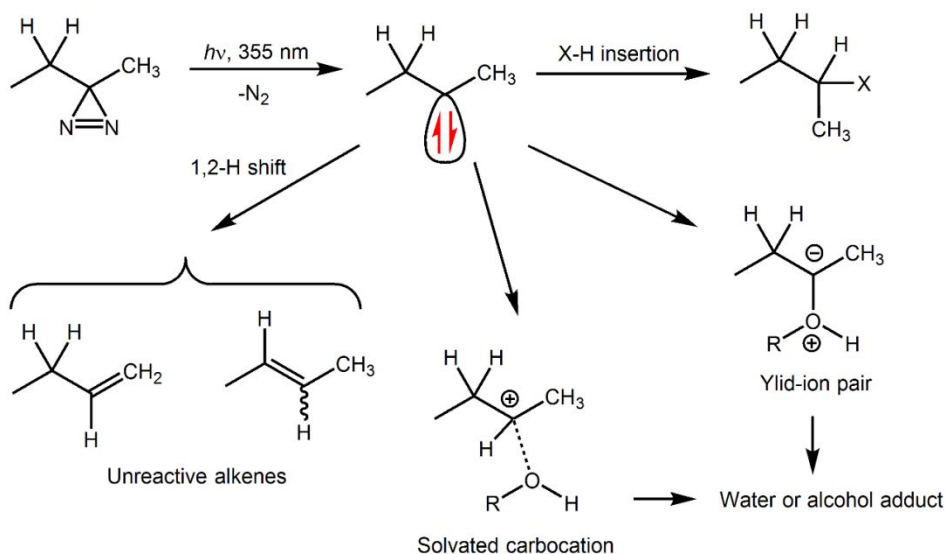
Scheme 4.   Competitive reactions of carbenes.

8

form of an alcohol or ether (Scheme 4).[58] An alternative pathway involves an ylid-ion pair that rearranges to an alcohol by proton migration. The chief side reaction of dialkylcarbenes is the fast competitive 1,2-hydrogen shift proceeding on a high picosecond to low nanosecond time scale and converting the carbene into an unreactive alkene.[60-64] Considering the model $(G(L*-N_2)GGK-NH_2 + H)^+$ ion, 1,2-H migrations from the carbene-flanking methyl and methylene groups have low activation energies, $E_a = 19$ and 31 kJ mol^{-1}, respectively and can proceed rapidly in thermal ions (Figure 5, right panel). Combining the calculated vibrational energy distribution at 310 K (Figure 5a) with RRKM-calculated rate constants for isomerization indicates a sub nanosecond half-life of the carbene in >50% ions (Figure 5b).[65] When a carbene to alkene isomerization occurs in an ion-molecule complex, its high exothermicity drives dissociation of the complex, leaving behind the crosslinked product as the main stable component whose structure can be further investigated by tandem mass spectrometry. We have taken another advantage of this side reaction and its kinetics to use it as an internal clock in our BOMD calculations of trajectories of non-covalent complexes. These are run on a 100 ps timescale to identify close contacts between the incipient carbene atom and the X–H bonds that can potentially undergo insertion. This has allowed us to correlate the computationally determined complex structures and their potential for amino acid cross linking with experimental results obtained by photodissociation and product sequence analysis by CID-MS^3.[38, 65-72]

Whereas carbene reactions with hydrocarbons have been studied in quite a detail, the effect of polar groups on the interaction with carbenes has received less attention and has been focused on small solvent molecules, such as water and alcohols. Experimental studies of peptide crosslinking in solution have chiefly been of a heuristic nature. A survey of crosslinking yields of a mixture of tryptic peptides with 3,3-azibutan-1-ol, 3,3-azibutan-1-amine, and 4,4-azipentanoic acid gave widely different results depending on the carbene source and amino acid residues in the peptide.[73] A solution cross-linking study has reported products that have been presumed to result from carbene coupling to aspartic and glutamic acid forming esters.[74] It has been suggested[74] that the coupling with carboxyl groups results from photochemical isomerization of diazirines to diazoalkanes.[75-77] However, as indicated by the Figure 4 data,[51] no diazirine isomerization has been detected in gas-phase photoleucine peptide ions by UV-vis and infrared multiphoton dissociation spectroscopies. Interestingly, an intramolecular cyclization between a carbene and a carboxyl group has not been observed in solution.[61]
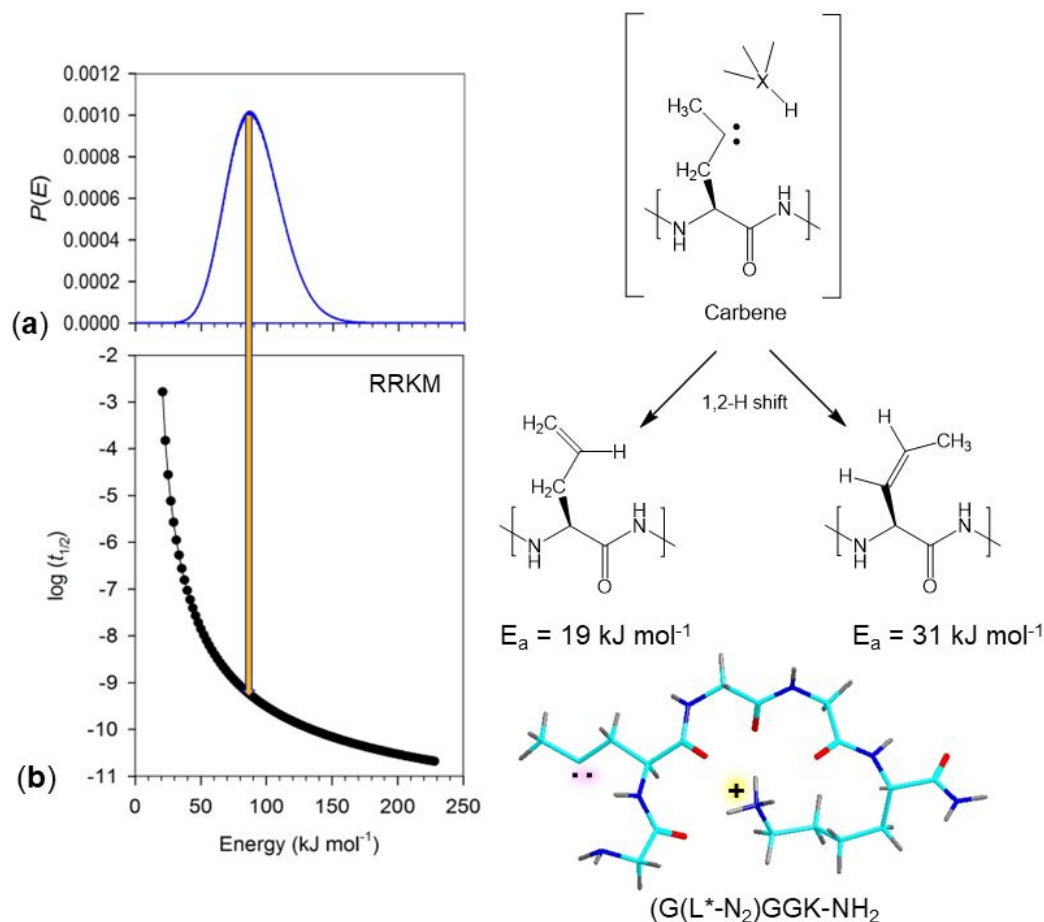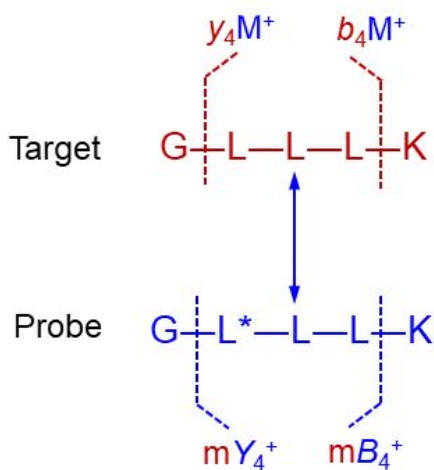
Figure 5. Left panel: (a) Vibrational energy distribution in $(G(L*-N_2)GGK-NH_2 + H)^+$ at 310 K. (b) Carbene half-life from RRKM unimolecular rate constants for 1,2-H migration. Right panel: Activation energies (E_a) for 1,2-H migration in $(G(L*-N_2)GGK-NH_2 + H)^+$. Reproduced from ref. 65 with permission from Elsevier, copyright (2019).

Peptide-Peptide Crosslinking

Gas-phase peptide-peptide crosslinking has been established in an early proof-of-the-concept study by Shaffer et al.[38] Those authors have observed site-specific crosslinking of diazirine-tagged probe peptides GL*LLK, GLL*LK, and GLLL*K with target peptides GLLLK in which the Leu residues were distinguished by ^{13}C labeling. The crosslinked sites in the target peptide were determined by sequencing the mass-selected crosslinks by CID-MS^3. Shafer et al. also have introduced a nomenclature for the crosslinked fragment ions (Figure 6). The target and probe peptides retained in the fragment ions are denoted by lower-case **m** and upper-case **M** letters, respectively. The fragment ions are denoted by y_n, Y_n, b_n and B_n for the corresponding cleavages

10

retaining the C-terminal and N-terminal sequences of the target and probe peptides. For example, y_1M^+ and b_1M^+ ions indicate the population of site-specific crosslinks at Lys-5 and Gly-1, respectively, in the target moiety of the crosslinked complex. Other fragment ions are less site-specific; for example, a y_4M^+ fragment ion combines crosslinks at Leu-2, Leu-3, Leu-4, and Lys-5, while excluding crosslink at Gly-1. Fragment ions resulting in backbone cleavage in both peptides are denoted analogously, e.g., $b_nB_m^+$, $b_nY_m^+$, $y_nB_m^+$, and $y_nY_m^+$, etc. The general conclusion from this study has been that crosslinking of these peptides achieved 19-21% yields of identifiable products according to CID-MS^3 sequencing. Crosslinking to GLLLK was found to chiefly occur near or at the C-terminal residues, Leu-4 and Lys-5, respectively.[38]

Figure 6. Fragment ion nomenclature in CID-MS^3 of crosslinked peptides.

In a related study, Nguyen *et al*. have examined crosslinking of GL*LLK, GLL*LK, and GLLL*K in non-covalent complexes with a library of proline and phenylalanine containing pentapeptides in which the Pro and Phe sequence positions were varied.[66] The experimental results were interpreted by carrying out computational analysis of contacts between the incipient carbene carbon atom in the probe peptide and atoms of the X—H bonds (X = C, N, O) in the target peptide. To that end, several low-energy conformational isomers were identified by BOMD and DFT for the (GLPMG + GLL*LK + H)$^+$ complexes that were further used as starting structures for 100 ps BOMD trajectories at 310 K. Upon contact analysis of 100000 snapshots in each trajectory, those in which the carbene and X atoms were within the shortest distance allowed by the van der Waals radii of the diazirine and X atoms were sorted out. The shortest distance was estimated as 4 Å.[38,66] The analysis predicted nearly 100% of diazirine contacts to occur within the Met and C-terminal Gly residues (Figure 7, top panel), which was consistent with the experimental crosslink distribution (Figure 7, bottom). Nguyen *et al*. also pointed out the limitations of CID-MS^3 sequencing in assigning the crosslinked residues, which due to the facile backbone fragmentation at the proline *N*-side[78] did not allow one to resolve the Pro-Met-Gly sites.
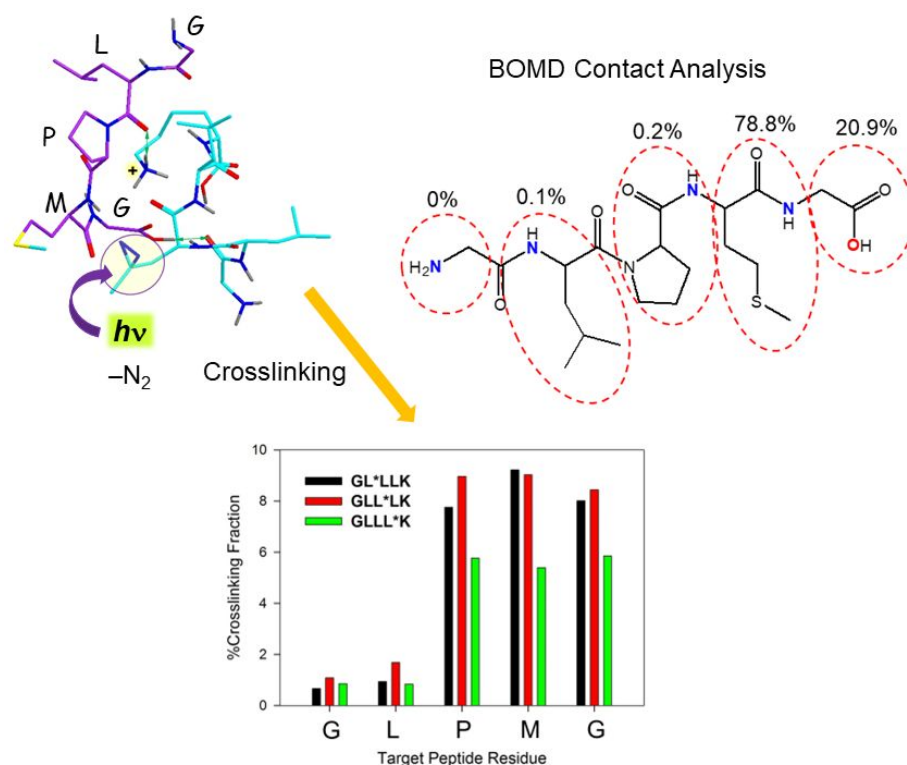
Figure 7. Crosslink distribution and BOMD contact analysis of the (GLPMG + GLL*LK + H)$^+$ complexes. Reproduced from ref. 66 with permission from American Chemical Society, copyright (2018) .

The portfolio of diazirine-tagged amino acid residues has been expanded by Pepin *et al*. who developed synthetic methods to selectively attach the 4,4-azipentyl group to the *N*-terminus, cysteine thiol, and lysine ε-amino group in the course of peptide synthesis.[67] This has been exploited by Liu *et al*. in a study of complexes between diazirine-tagged CAQK and several peptides.[68] CAQK is a small peptide that had been found to selectively bind to injured mouse and human brain, where its target was presumed to be chondroitin sulfate proteoglycan 4 precursor (CSPG4) that was upregulated in brain injuries.[79] However, the peptide binding mechanism and even the binding protein had not been determined in the brain study. Hence, CAQK represented a suitable target for a *de novo* binding study of representative peptide motifs from CSPG4 using gas-phase crosslinking combined with computational data analysis. To that end, Liu *et al*. used a library approach in which CAQK peptide probes that were specifically labeled with the 4,4-azipentyl group in cysteine, lysine, and at the *N*-terminus were used to generate and study non-covalent complexes with CSPG4 peptide motifs LLSPGH, ALLVRST, and FGENHL A detailed UVPD-CID-MS^3 investigation of the CAQK complexes with LLSPGH, LLSPGH-NH$_2$ and *N*-Ac-

LLSPGH has revealed 22-28% crosslinking efficiency for C*AQK binding to LLSPGH and *N*-Ac-LLSPGH, whereas the peptide amide showed only a 4% yield. BOMD and DFT analysis of the $(CAQK + H)^+$ and $(C*AQK + H)^+$ ion structures indicated that the *S*-4,4-azipentyl group had only a minor effect on the free peptide conformation that in each case was dominated by internal solvation of the protonated lysine ε-amine group.   Liu et al. have carried out a detailed computational analysis of the $(C*AQK + LLSPGH + H)^+$ complexes that yielded three low-energy structures (<u>Figure 8</u>) that were within 7 kJ mol^{-1} and differed in the component binding and the position of the diazirine ring (denoted with an asterisk in Figure 8).
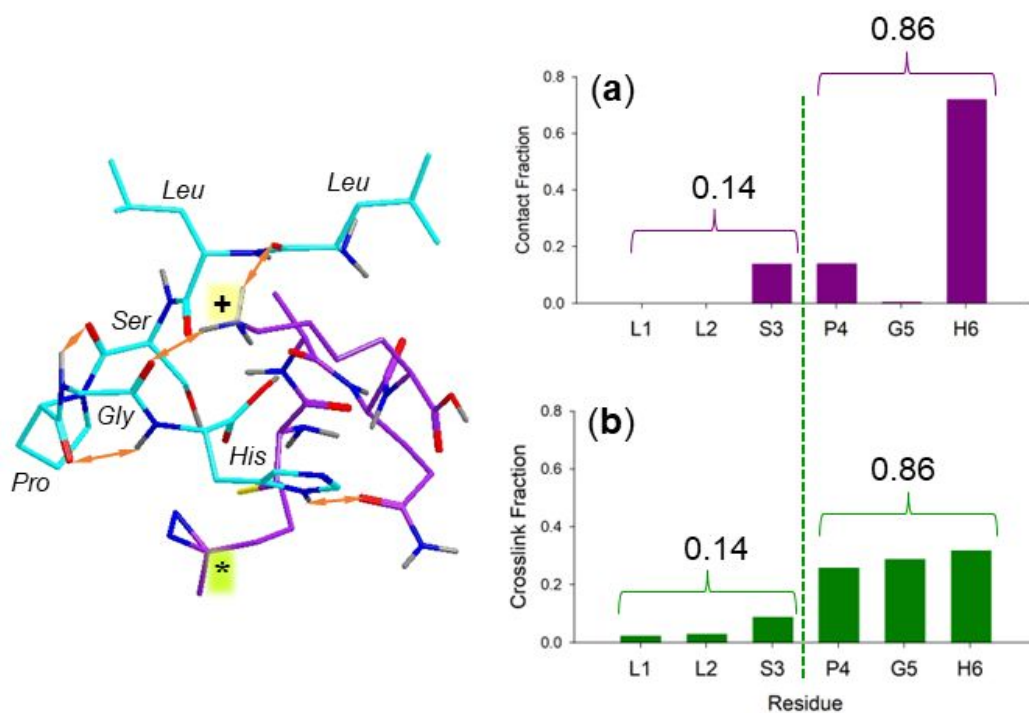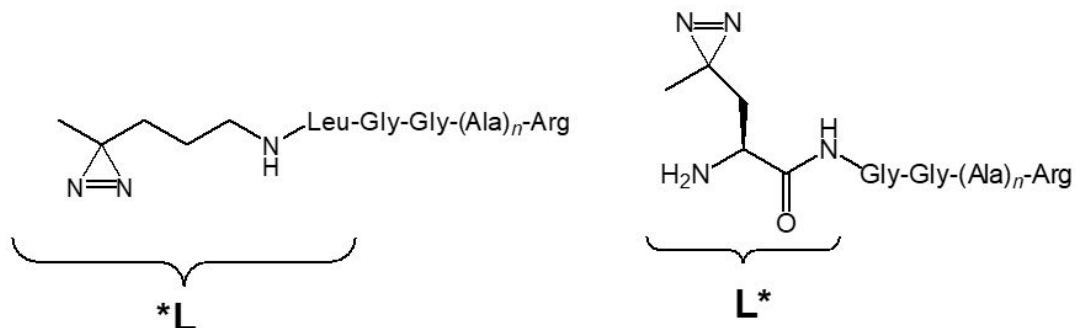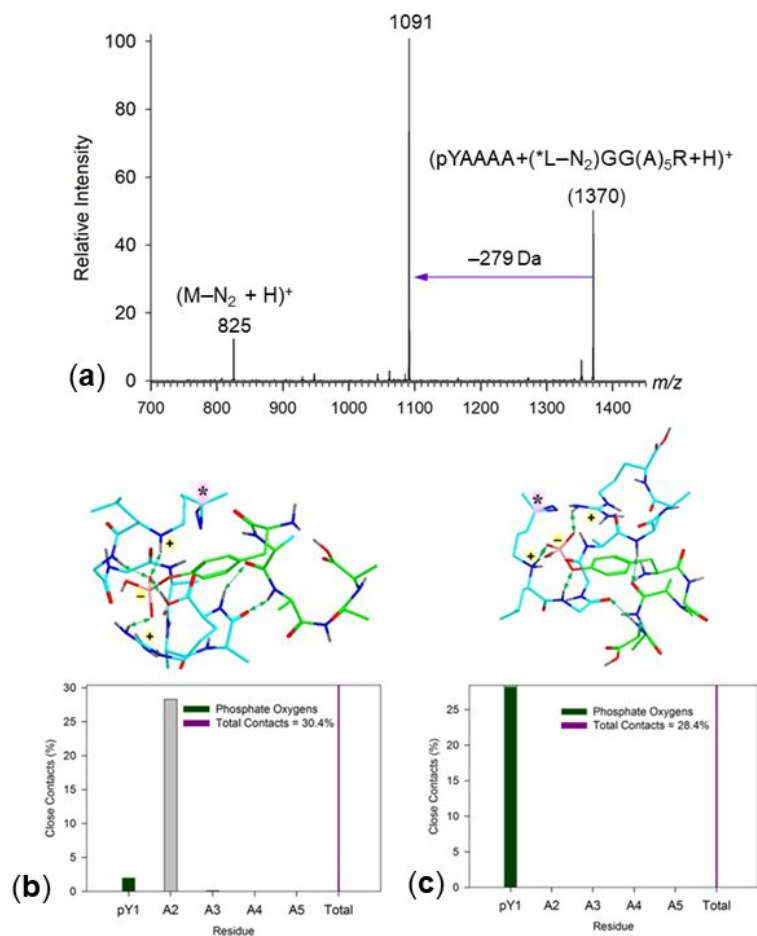

Figure 8. Left panel: Low-energy structure of the $(C*AQK + LLSPGH + H)^+$ complex. The carbon atoms colors are cyan and purple in LLSPGH and C*AQK, respectively. Right panel: (a) Contact analysis of 100 ps trajectories. (b) Experimental crosslink distribution.[68]

The authors have found the best match for the structure shown in Figure 8 that upon analysis gave 86% combined contacts with the Pro-Gly-His residues. This was matched by the fraction of combined crosslink sites based on the y_1M, y_2M and y_3M fragment ions resulting from the target peptide sequencing. Again, the facile backbone dissociation at Pro hampered more specific crosslink assignment within the Pro-Gly-Lys sequence. The fitting structure showed a tightly folded β-turn at the LLSPGH proline residue that shaped the complex into an intertwined, yin-

yang-like shape that was chiefly maintained by strong hydrogen bonds of the Lys NH_3^+ to the His-6-COOH, Gly-5, and Leu-1 carbonyls. The authors suggested that a similar β-turn cleft in LLSPGH may play a role in the CAQK binding to proteins.[68]

Carbene-based crosslinking has also been employed to study non-covalent binding of amyloid peptide motifs Gly-Asn-Asn-Gln-Gln-Asn-Tyr in gas-phase complexes in which one component was tagged with the 4,4-azipentyl group at the N-terminus.[69] The gas-phase complexes, which included all four combinations of carboxyl and amide C-terminal groups, were formed at only ca. 0.2% yields relative to the monomeric peptide ions and showed only 0.8-4.5% total crosslinking efficiency. Similar low yields (0.6-3.5%) were obtained for gas-phase complexes of phosphopeptides pXAAAA and N-Ac-pXAAAA (X = Ser, Thr, Tyr) and arginine-containing peptides *LGG(A)$_n$R carrying the 4,4-azipentyl tag at the N-terminus.[65] Even lower yields (<0.1%) were obtained for complexes with L*GG(A)$_n$R that were tagged in photoleucine. These results were contrary to previous reports that had claimed that stable phosphopeptide-arginine complexes were produced in the gas phase by soft-ionization methods.[80,81]

*L

L*

Despite their low-yield formation, the gas-phase phosphopeptide complexes with *LGG(A)$_n$R showed 11-92% crosslink efficiencies that increased with the length of the probe peptide, n = 3-5. In particular, CID-MS^3 of the (pXAAAA + *LGG(A)$_n$R + H)$^+$ complexes showed a dominant loss of crosslinked neutral fragments that originated from the phosphopeptide moiety (Figure 9a). The complex ion structure and dynamics were studied for (pYAAAA + *LGGAAAR + H)$^+$ that included several types of protonation isomers differing in the charge distributions between the phosphopeptide (neutral or phosphate anion) and probe peptide (Arg-protonated or doubly protonated). The lowest energy structures, which were all zwitterions (Figure 9b,c), displayed frequent contacts with the phosphopeptide N-terminal residues indicating a high probability for crosslinking at these residues.[65]

Figure 9. (a) UVPD-CID-MS^3 spectrum of the (pYAAAA+(*L–N$_2$)GG(A)$_5$R+H)$^+$ complex. (b,c) Optimized structures of the lowest-energy (pYAAAA+(*L–N$_2$)GG(A)$_3$R+H)$^+$ complexes with contact analysis of 100 ps BOMD trajectories. Green bars indicate contacts with phosphate oxygens, the gray bar is for contacts with C–H bonds.[65]

Peptide-Nucleotide Crosslinking.

Crosslinking of oligonucleotides that were tagged with diazirine in guanine and cytosine has also been developed to study protein-DNA interactions and shown to achieve up to 30% yields of crosslinks.[82] Liu and Turecek have used the diazirine-tagged CAQK peptides, *CAQK, C*AQK, and CAQK*, to investigate binding to a series of dinucleotides, d*AA*, d*AT*, d*GG*, d*GC*, and d*CG*

in singly charged gas-phase complexes.[70] Gas-phase crosslinking showed strong dependence of crosslink yields on the dinucleotide composition. In particular, the dinucleotides containing guanine showed 90-98% yields after photodissociation, out of which 18-47% were identified as crosslinks by CID-MS³. Interestingly, while complexes of d*AA* and d*AT* showed more extensive dissociation upon diazirine photolysis, the surviving $(m + M-N_2 +H)^+$ complexes (m = dinucleotide, M = photopeptide) consisted of >50% of crosslinked products. CID of the crosslinks
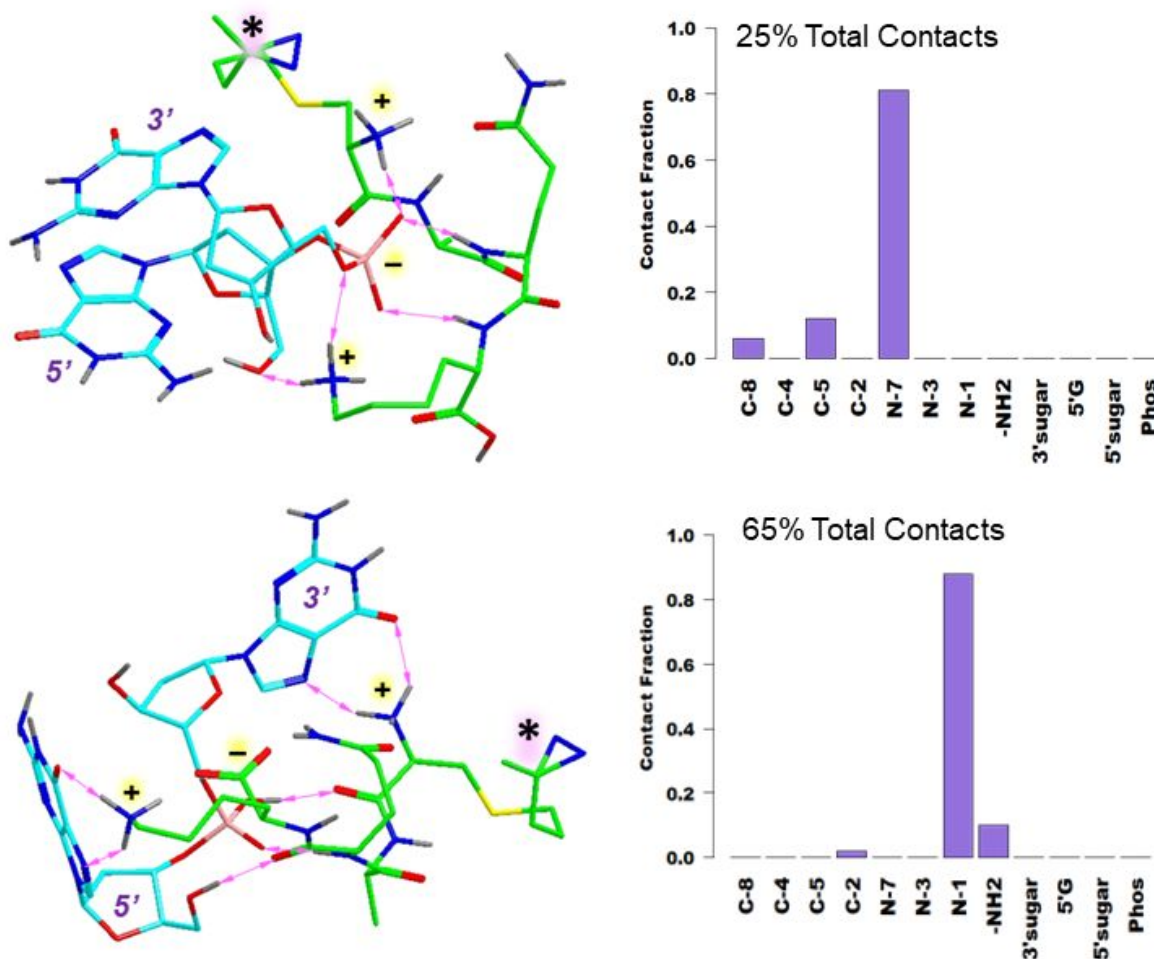

Figure 10. Lowest-energy (d*GG* + C*AQK + H)⁺ complexes and distribution of contacts at *3'*-guanine positions in 100 ps BOMD trajectories at 310 K. Reproduced from ref. 70 with permission from American Chemical Society, copyright (2019).

unambiguously showed standard dissociations in the dinucleotide moieties, such as loss of nucleobase and backbone cleavages while peptide fragmentations were virtually absent. Structure analysis was carried out for the (d*GG* + C*AQK + H)⁺ complexes where BOMD + DFT calculations starting from multiple initial structures revealed at least 16 fully optimized structures

that were within a narrow range of Gibbs energies that would permit isomer coexistence in a gas-phase equilibrium (Figure 10). Overall, the calculated energies favored zwitterionic isomers of the (Cys$^+$, Lys$^+$, COO$^-$)$^+$ and (Cys$^+$, Lys$^+$, phosphate$^-$)$^+$ types. Interestingly, zwitterionic isomers were also favored by calculations that included ion solvation by water.[70] Analysis of long (100 ps) BOMD trajectories of the low-energy complexes revealed numerous contacts with atoms of the 3'-nucleobase, although their dynamics differed. For example, the low Gibbs-energy phosphate zwitterion (Figure 10, top structure) showed the incipient carbene and 3'-guanine N-7 atoms in close proximity already in the fully optimized structure referring to 0 K. In contrast, the carboxylate zwitterion (Figure 10, bottom structure), in which the incipient carbene was remote from the 3'-guanine at 0 K, attained numerous contacts with the 3'-guanine N-1 position as a result of dynamic nuclear motion at 310 K (Figure 10).

Peptide-Ligand Crosslinking

A different technique had to be employed to analyze the structures of gas-phase complexes of diazirine-tagged D- and L-adrenaline with the binding peptide motif of the β-adrenogenic receptor (β$_2$AR).[71] The main peptide motif in catechol binding to (β$_2$AR) is the S203-Y209 sequence, Ser-Ser-Ile-Val-Ser-Phe-Tyr, which is located on the extracellular side of the protein α-helix strand.[83,84] This interaction has also been probed in the gas-phase complex of L-adrenaline with N-Ac-Ser-Ser-Ile-Val-Phe-NHCH$_3$ in a study that used UV-infrared spectroscopy.[85] UV-IR has allowed the authors to distinguish two groups of complexes in which adrenaline was bound to the peptide by the catechol OH groups. However, a more detailed structure assignment was made difficult because of the lack of characteristic vibrational modes.[85] In their crosslinking study, Liu et al. have taken advantage of the relative tolerance of β$_2$AR for binding with adrenaline derivatives that were modified in the side chain.[83,86] This has allowed Liu et al. to introduce the 4,4-azipentyl group into the side-chain amine in D- and L-adrenaline and use the modified adrenalines for a study of photodissociation crosslinking in complexes with N-Ac-Ser-Ser-Ile-Val-Ser-Phe-Tyr-NH$_2$.[71] While complexes with the D- and L-adrenaline derivatives were formed readily by electrospray, UVPD and UVPD-CID of the photodissociation intermediates resulted in complete dissociation to the components, indicating there was no carbene-based crosslinking to the peptide. This raised the question of the complex structure and dynamics. Liu et al. have used high-resolution cyclic ion mobility mass spectrometry (c-IMS)[41] to probe the composition of the

complexes before photodissociation. c-IMS measurements have shown single peaks for the D- and L-adrenaline complexes, indicating their structure homogeneity. The measured collision cross sections (CCS_{exp}) in nitrogen were matched within 1% by CCS_{calc} that was calculated for a low-energy complex (Figure 11) while excluding other isomers. The complex showed hydrogen bonds of the catechol hydroxyls to the Ser-2 and Ser-5 hydroxyls as well as the Ser 5 amide (Figure 11) which were consistent with specific binding by the peptide. However, analysis of BOMD trajectories revealed frequent contacts of the incipient carbene with the C-terminal amide that,
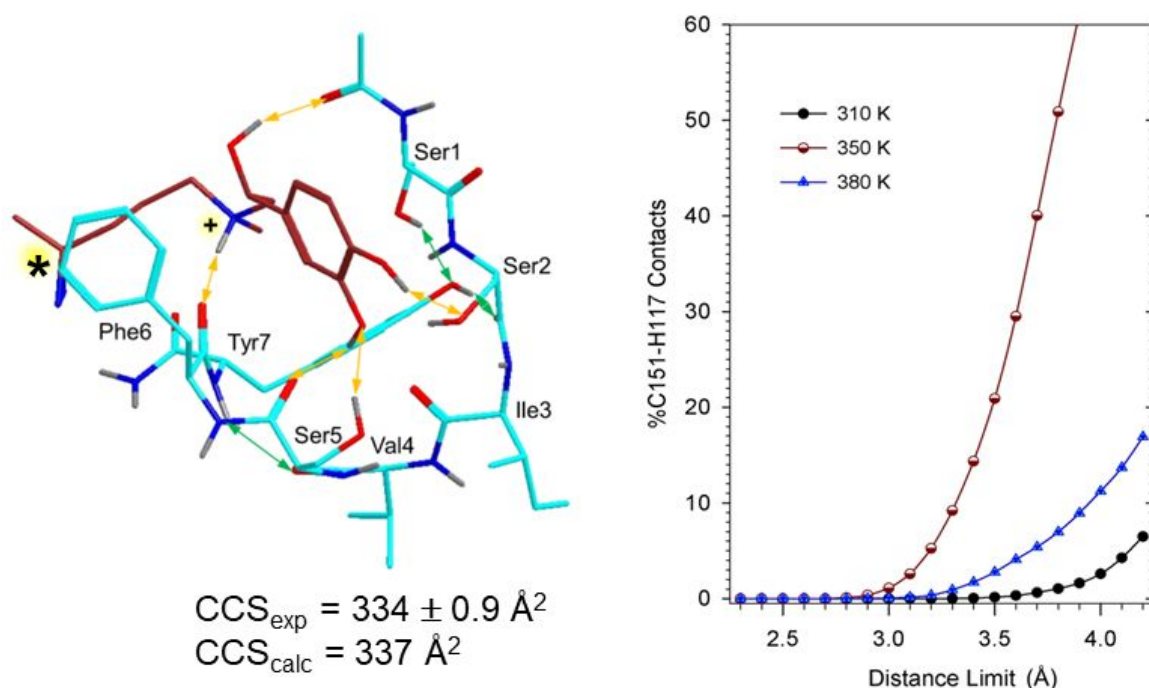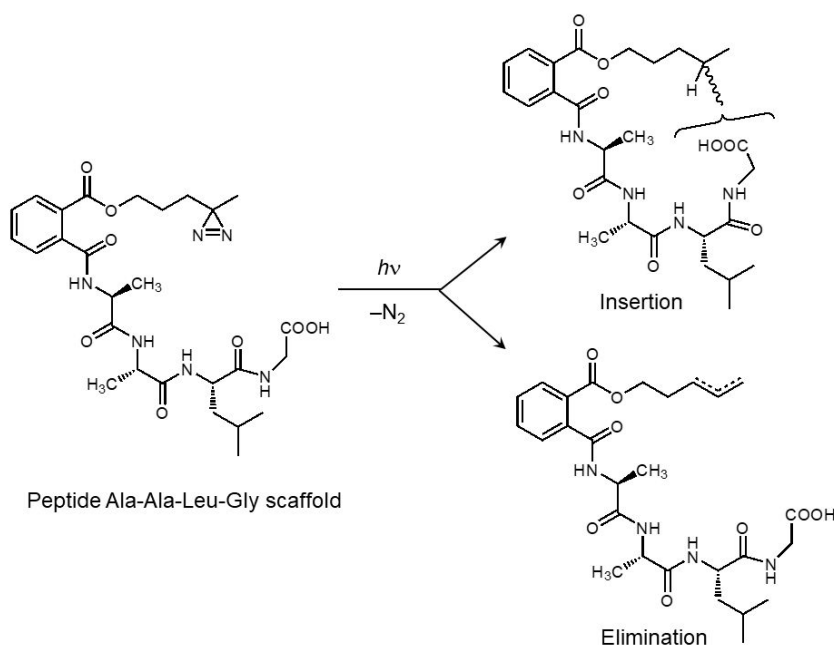

Figure 11. Left panel: DFT-optimized geometry of a low-energy complex of diazirine-tagged L-adrenaline with N-Ac-Ser-Ser-Ile-Val-Ser-Phe-Tyr-NH$_2$. The incipient carbene is denoted by an asterisk. Right panel: Contact frequency between the carbene atom (C151) and C-terminal amide hydrogen (H117) as a function of distance limit in BOMD trajectories. Reproduced from ref. 71 with permission from American Chemical Society, copyright (2021).

however, did not result in crosslinking. On the basis of energy analysis and dynamics of smaller adrenaline ion models, Liu *et al.* have suggested that carbene insertion into the amide N–H bonds was associated with an energy barrier that favored the competitive carbene isomerization by 1,2-hydrogen migration.[71]

The results from the L-adrenaline study have raised the general question of crosslinking to polar X–H bonds that has been addressed with using peptide-diazirine scaffolds. In these synthetic

constructs, the peptide and diazirine carrier, such as the 4,4-azi pentyl group, are mounted on a covalent scaffold that limits the conformational motion of both moieties.[72] Photochemical crosslinking between the carbene intermediate and peptide bonds is detected by CID-MS[3] analysis of the products. A scaffold of the Ala-Ala-Leu-Gly tetrapeptide with the phthalate linker is shown in Scheme 5.

Peptide Ala-Ala-Leu-Gly scaffold

Insertion

Elimination

Scheme 5. Photodissociation and carbene reactions in the AALG scaffold.

Compared to non-covalent complexes, the use of scaffolds for crosslinking studies brings several advantages. First, gas-phase scaffold ions are generated abundantly by electrospray ionization because there are no issues with their stability. Second, products of insertion and elimination are readily distinguished and identified

by comparing the CID-MS[3] data of the photoproducts with those of synthetic standards, such as olefins or macrocyclic lactones. Third, peptide sequence variants, derivatization, and H/D exchange are feasible to be used for mechanistic studies. Photodissociation of scaffolds with nonpolar AALG, ALAG, and LAAG peptides has been found to give 21-26% crosslink yields, which was comparable to those for peptide-peptide complexes.[38,66] Scaffolds with AAPG and AAHG peptides gave lower yields.[72] The *C*-terminal carboxyl was found to play an important role in crosslinking, as established by carboxyl blocking as an ester and by H/D exchange. The H/D exchange experiment consisted of exhaustive exchange of all active protons in the AALG scaffold into the D cycle, followed by photodissociation. The products were exhaustively back exchanged into the H cycle and analyzed by CID-MS[2]. The spectra unambiguously showed incorporation of a single deuterium in a nonexchangeable position within the pentyl chain, which was only possible by X–D insertion into the carbene by crosslinking. The structure assignment of the photoproduct

was finalized by CID-MS^2 of an authentic macrocyclic lactone that was synthesized, and its spectrum showed the same features as that of the photoproduct.[72] This way, the resolution in the product structure analysis was augmented to achieve identification of individual amino acid bonds that were involved in crosslinking.

Concluding Remarks on Carbene Crosslinking

Carbenes generated from diazirines have been the workhorse in crosslinking studies, as shown by both solution studies[1] and the above-described examples. The precursor diazirines are readily introduced via modified amino acid residues into synthetic peptides or proteins. Gas-phase ion complexes can be formed from components of an even low binding affinity in solution, thus providing a range of combinations for library-type binding studies. However, the applications to gas-phase crosslinking face a few drawbacks, both fundamental and technical. One of the fundamental issues is that binding in gas-phase complexes is affected by the absence of solvent and presence of charges that are solvated internally, thus potentially affecting the conformations of the complex components. This effect has to be considered by careful examination of ions from the individual components.[68] Computations of structures and energies at the DFT level, including all relevant protonation isomers and conformers, are limited by the size of the systems that could be addressed. The current limit, estimated at ca. <500 atoms, is likely to move up as a result of technology advances, but at present protein complexes are out of range of de novo analysis. One of the technical limitations is the very low molar absorptivity of the $\pi_{xy} \rightarrow \pi_z^*$ transition to the first excited singlet state of the diazirine (Figure 3), so that achieving photodissociation conversions that would be suitable for further product analysis typically requires multiple (>10) laser pulses. Although weak absorption is not a major issue in solution studies where irradiation times going for hours are common, it represents an impediment in gas-phase studies by prolonging data acquisition. The high reactivity of the carbenes, including their self-destruction by 1,2-hydrogen migration, can be detrimental to crosslinking reactions that are slowed down by energy barriers to insertion or conformational motion. In addition, the indiscriminate nature of carbene reactions can make it difficult to carry out structure and mechanistic studies of crosslinking in polyatomic biomolecules. Finally, the localization of crosslinks in peptides critically depends on the ability to obtain high sequence coverage of the $\boldsymbol{y}_n$M and $\boldsymbol{b}_m$M fragment ions by collision-induced dissociation. This applies to crosslinking in the gas-phase as well as in solution when

followed by bottom-up peptide analysis. Amino acid residues that are prone to facile backbone cleavage (Pro, Glu) are detrimental in this respect in that they decrease the resolution of the crosslink positional assignment.

Beyond Carbene Crosslinking

To address some of the above-mentioned issues, we have recently been exploring the possibility of using other reactive intermediates as gas-phase crosslinkers that would avoid the diazirine-carbene drawbacks. Nitrile imines[87] have been suggested for derivatization of peptides and proteins[88] via the well known [3+2] cycloadditions with dipolarophiles.[89] Nitrile imines are readily available by thermolysis or photolysis of 2,5-diaryl tetrazoles which can be readily introduced as tags into peptides or other biomolecules.[88] 2,5-Diphenyltetrazole has a major absorption band with a λ_{max} at 255 nm and $\varepsilon \cong 2 \times 10^4$ L mol^{-1} cm^{-1} that was measured by Blanksby, Trevitt, *et al.* in gas-phase ions.[90] This makes tetrazole a strong chromophore for photodissociation. Preliminary results with photodissociation of tetrazole-tagged peptides have shown a potential for crosslinking and structure elucidation. Figure 12 shows an Ala-Ala-Ala-Gly peptide built on a *cis*-1,2-cyclohexane scaffold that carries the 5-phenyl-2-phenyl-(4-carboxamide)tetrazole
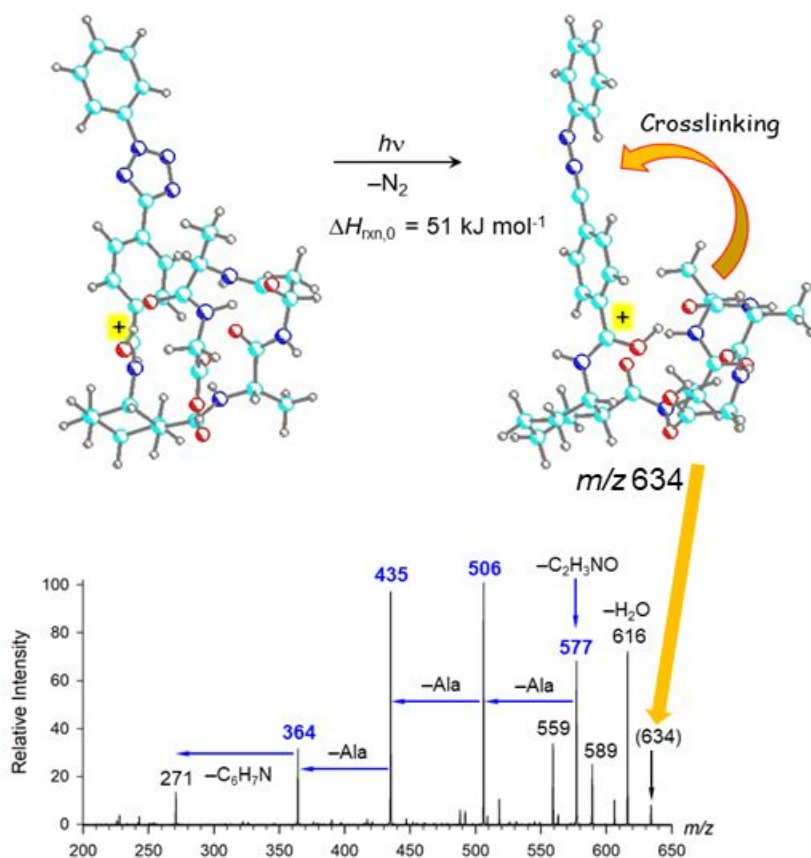

Figure 12. Top: M06-2X/6-31+G(d,p) optimized low energy structures of AAAG-tetrazole scaffold ions. Bottom: UVPD-CID-MS^3 spectrum of the photoproduct after loss of N$_2$. Blue colored fragment ions indicate crosslinking. The *m/z* 559 fragment ion (loss of GlyOH) is indicative of an open peptide chain.

group. Photodissociation of the gas-phase cations at 250 nm produced the transient nitrile imines that were probed by CID-MS^3 (Figure 12, bottom panel). The spectrum showed >90% of fragment ions produced by loss of internal peptide residues that were indicative of peptide cyclization[91,92] to the nitrile imine. This was distinctly different from dissociations of tetrazole-peptide conjugates that showed standard sequence ions of the b_n and y_n type, and thus the internal fragments formation from the photoproducts was unambiguous evidence of nitrile imine crosslinking. The low-energy optimized structures (Figure 12) indicated that only the *C*-terminal Gly was sterically accessible for reacting with the nitrile imine group. The calculated reaction enthalpy for the nitrile imine formation by loss of N_2 upon absorption of a 250 nm (4.96 eV, 479 kJ mol^{-1}) photon, $\Delta H_{rxn,0} = 51$ kJ mol^{-1} by M06-2X/6-311++G(2d,p) (Figure 12), indicated that the nitrile imine intermediate was produced with a substantially increased internal energy. This excitation can be estimated from the energy balance as $E_{exc} \leq 479 - 51 = 428$ kJ mol^{-1} where the $\leq$ sign accounts for the translational energy of the departing N_2 molecule. The high internal energy from photodissociation is presumed to drive subsequent reactions of the nitrile imine to proceed on the millisecond time scale of the experiment and result in efficient crosslinking, as evidenced by the CID-MS^3 data. These and other recent data indicate that nitrile imine reactions resulting in cyclization and crosslinking are common in peptide conjugates and have also been observed for non-covalent complexes with nucleotides. Thus it appears that nitrile imine-based crosslinking of biomolecular ions can have a tremendous potential for the exploration and applications in biomolecular ion structure analysis, and is currently being explored to determine the functional group selectivity, crosslink structures, and mechanism.

Conflict of interest

There are no conflicts to declare.

Acknowledgments

References

(1) L. Piersimoni, P. L. Kastritis, C. Arlt and A. Sinz, *Chem. Rev.* 2022, **122**, 7500.

(2) Y. Sun, N. M. Hayes, A Periasamy, M. W. Davidson and R.. N. Day, *Methods Enzymol.* 2012, **504**, 371.

(3) Y. Sun, R. N. Day and A. Periasamy, *Nature Protoc.* 2011, **6**, 1324.

(4) C. Uetrecht, R, J. Rose, E. van Duijn, K. Lorenzen and A. J. Heck, *Chem. Soc. Rev.* 2010, **39**, 1633.

(5) J. Wang, X. Zuo, P. Yu, H. Xu, M. R. Starich, D. M. Tiede, B. A. Shapiro, C. D. Schwieters and Y.-X. Wang, *J. Mol. Biol.* 2009, **393**, 717.

(6) A. Singh, E. R. Thornton and F. H. Westheimer, *J. Biol. Chem.* 1962, **237**, PC3006.

(7) J. R. Knowles, *Acc. Chem. Res*. 1972, **5**, 155.

(8) G. W. J. Fleet, R. R. Porter and J. R. Knowles, *Nature* (London) 1969, **224**, 511.

(9) R. A. G. Smith and J. R. Knowles, *J. Am. Chem. Soc.* 1973, **95**, 5072.

(10) J. Das, *Chem. Rev.* 2011, **111**, 4405.

(11) R. E. Galardy, L. C. Craig, J. D. Jameison and M. P. Printz, *J. Biol. Chem.* 1974, **249**, 3510.

(12) J. C. Kauer, S. Erickson-Viitanen, H. R. Wolfe, Jr., and W. F. DeGrado, *J. Biol. Chem*. 1986, **261**, 10695.

(13) G. Dorman and G. D. Prestwich, *Biochemistry* **1**994, **33**, 5661.

(14) N. Hino, Y. Okazaki, T. Kobayashi, A. Hayashi, K. Sakamoto and S. Yokoyama, *Nature Methods* 2005, **2**, 201.

(15) M. T. H. Liu, *Chemistry of Diazirines*; Vol. I and II. CRC Press, Boca Raton (1987).

(16) H. M. Frey and I. D. R.Stevens, *J. Chem. Soc.* **1963**, 3514.

(17) D. H. R. Barton, J. C. Jaszberenyi, E. A. Theodorakis and J. H. Reibenspies, *J. Am. Chem. Soc.* 1993, **115**, 8050.

(18) S. M. Korneev, *Eur. J. Org. Chem.* **2011**, 6153.

(19) M. Hashimoto and Y. Hatanaka, *Eur. J. Org. Chem.* **2008**, 2513.

(20) L. Dubinsky, P. Bastiaan, B. P. Kroma nd M. M. Meijler, *Bioorg. Med. Chem.* 2012, **20**, 554.

(21) A. B. Kumar, J. M. Anderson and R. Manetsch, *Org. Biomol. Chem.* 2011, **9**, 6284.

(22) N. G. Rondan, K. N.Houk and R. A. Moss, *J. Am. Chem. Soc.* 1980, **102**, 1770.

(23) W. von Doering and L. H. Knox, *J. Am. Chem. Soc*. 1961, **83**, 1989.

(24) S. Sakai, *Int. J. Quant. Chem.* 1998, **70**, 291.

(25) M. S. Platz, *Acc. Chem. Res.* 1988, **21**, 236.

(26) J. L. Mieusset and U. H. Brinker, *J. Org. Chem*. 2008, **73**, 1553.

(27) V. P. Senthilnathan and M. S. Platz, *J. Am. Chem. Soc.* 1980, **102**, 7637.

(28) L. M. Hadel, V. M. Maloney, M. S. Platz, W. G. McGimpsey and J. C. Scaiano, *J. Phys. Chem.* 1986, **90**, 2488.

(29) B. B. Wright, V. P. Senthilnathan, M. S. Platz and C. W. McCurdy, Jr., *Tetrahedron Lett*. 1982, **23**, 833.

(30) Y. Tanaka, M. R. Bond and J. J. Kohler, *Mol. BioSyst*. 2008, **4**, 473.

(31) J. W. Chin, A. B. Martin, D. S. King, L. Wang and P. G. Schultz, *Proc. Natl. Acad. Sci. U. S. A*. 2002, **99**,11020.

(32) J. W. Chin and P. G. Schultz, *Chembiochem*, 2002, **3**, 1135.

(33) H. S. Lee, R. D. Dimla and P. G. Schultz, *Bioorg. Med. Chem. Lett*., 2009, **19**, 5222.

(34) R. Miazaki, Y. Akiyama and H. Mori, *Biochim. Biophys. Acta General Subjects* 2020, **1864**, 129317.

(35) M. Suchanek, A. Radzikowska and C. Thiele, *Nat. Methods* 2005, **2**, 261.

(36) T. Yang, X.-M. Li, X. Bao, Y. M. E. Fung and D. Li, *Nature Chem.Biol.* 2016, **12**, 70.

(37) Y. Aydin and I. Coin I. *Protein Sci.* 2023, **32**, e4637

(38) C. J. Shaffer, P. C. Andrikopoulos, J. Řezáč, L. Rulíšek and F. Tureček, *J. Am. Soc. Mass Spectrom.* 2016, **27**, 633.

(39) J. Řezáč, J. Fanfrlík, D. Salahub and P. Hobza, P. *J. Chem. Theory Comput.* 2009, **5**, 1749.

(40) J. Řezáč, *J. Comput. Chem.* 2016, 37, 1230.

(41) K. Giles, J. Ujma, J. Wildgoose, S. Pringle, K. Richardson, D. Langridge and M. A. Green, *Anal. Chem.* 2019, **91**, 8564.

(42) S. Lee, S. J. Valentine, J. P. Reilly and D. E. Clemmer, *J. Am. Chem. Soc.* 2011, **133**, 15834.

(43) W. M. McGee and S. A. McLuckey, *Proc. Natl. Acad. Sci. U. S. A.* 2014, **111**, 1288.

(44) M. C. S. Kit and I. K. Webb, *Anal. Chem.* 2022, **94**, 13301.

(45) A. Marek and F. Tureček, *J. Am. Soc. Mass Spectrom.* 2014, **25**, 778.

(46) A. Marek, R. Pepin, B. Peng, K. J. Laszlo, M. F. Bush and F. Tureček, *J. Am. Soc. Mass Spectrom.* 2013, **24**, 1641.

(47) A. Marek, C. J. Shaffer, R. Pepin, K. Slováková, K. J. Laszlo, M. F. Bush and F. Tureček, *J. Am. Soc. Mass Spectrom.* 2015, **26**, 415.

(48) C. J. Shaffer, A. Marek, H. T. H. Nguyen and F. Tureček, *J. Am. Soc. Mass Spectrom.* 2015, **26**, 1367.

(49) R. Pepin and F. Tureček, *J. Phys. Chem. B*, 2015, **119**, 2818.

(50) M. Heymann, H. Hippler and J. Troe, *J. Chem. Phys.* 1984, **80**, 1853.

(51) C. J. Shaffer, J. Martens, A. Marek, J. Oomens and F. Tureček, *J. Am. Soc. Mass Spectrom.* 2016, **27**, 1176.

(52) W. Kirmse, *Adv. Carbene Chem.* 2001, **3**, 1.

(53) T. H. Stein, M. Vasiliu, A. J. Arduengo, A. J., III, and D. A. Dixon, *J. Phys. Chem. A* 2020, **124**, 6096.

(54) P. M. Warner and I. S. Chu, *J. Am. Chem. Soc.* 1984, **106**, 5366.

(55) E. J. Dix and J. L. Goodman, *J. Phys. Chem*. 1994, **98**, 12609.

(56) J. Peon, D. Polshakov and B. Kohler, *J. Am. Chem. Soc.* 2002, **124**, 6428.

(57) A. A. A. Abu-Saleh, M. Almatarneh and R. A. Poirier, *Chem. Phys. Lett*. 2018, **698**, 36.

(58) W. Kirmse, T. Meinert, D. A. Modarelli and M. S. Platz, *J. Am. Chem. Soc*. 1993, **115**, 8918.

(59) B. B. Wright and M. S. Platz, *J. Am. Chem. Soc*. 1984, **106**, 4175.

(60) J. E. Jackson, N. Soundararajan, W. Whie, W., M. T. H. Liu, R. Bonneau and M. S. Platz, *J. Am. Chem. Soc*. 1989, **111**, 6874.

(61) I. D. R. Stevens, M. T. H. Liu, N. Soundararajan and N. Paike, *Tetrahedron Lett*. 1989, **30**, 481.

(62) M. H. Sugiyama, S. Celebi and M. S. Platz, *J. Am. Chem. Soc*. 1992, **114**, 966.

(63) S. Celebi, S. Leyva, D. A. Modarelli and M. S. Platz, *J. Am. Chem. Soc*. 1993, **115**, 8613.

(64) J. P. Pezacki, P. Couture, J, A. Dunn, J. Warkentin, P. D Wood, J. Lusztyk, F. Ford and M. A. Platz, *J. Org. Chem.* 1999, **64**, 4456.

(65) H. T. H. Nguyen, S. R. Huang, Y. Liu, Y. Liu, J. A. Korn and F. Turecek, *Int. J. Mass Spectrom.* 2019, **435**, 259.

(66) H. T. H. Nguyen, P. C. Andrikopoulos, L. Rulíšek, C. J. Shaffer and F. Tureček, *J. Am. Soc. Mass Spectrom.* 2018, **29**, 1706.

(67) R. Pepin, C. J. Shaffer and F. Tureček, *J. Mass Spectrom.* 2017, **52**, 557.

(68) Y. Liu, Z. Ramey and F. Tureček, *Chem. Eur. J.* 2018, **24**, 9259.

(69) S. R. Huang, Y. Liu and F. Tureček, *Phys. Chem. Chem. Phys.* 2019, **21**, 2046.

(70) Y. Liu and F. Tureček, *J. Am. Soc. Mass Spectrom.* 2019, **30**, 1992.

(71) Y. Liu, Y. Liu, M. Nytka, S. R. Huang, K. Lemr and F. Turecek, *J. Am. Soc. Mass Spectrom.* 2021, **32**, 1041.

(72) H. Zhu, V. Zima, E. Ding and F. Tureček, *J. Am. Soc. Mass Spectrom.* 2023, **34**, 763.

(73) D. S. Ziemianowicz, R. Bomgarden, C. Etienne and D. C. Schriemer, *J. Am. Soc. Mass Spectrom.* 2017, **28**, 2011.

(74) C. Iacobucci, M. Goetze, C. Piotrowski, C. Arlt, A. Rehkamp, C. Ihling, C. Hage and A. Sinz, *Anal. Chem.* 2018, **90**, 2805.

(75) S. M. Korneev, *Eur. J. Org. Chem.* **2011**, 6153.

(76) M. J. Amrich and J. A. Bell, *J. Am. Chem. Soc.* 1964, **86**, 292.

(77) E. Voigt and H. Meier, *Chem. Ber.* 1975, **108**, 3326.

(78) T. Vaisar and J. Urban, *J. Mass Spectrom.* 1996, **31**, 1185.

(79) A. P. Mann, P. Scodeller, S. Hussain, J. Joo, E. Kwon, G. B. Braun, T. Molder, Z.-G. She, V. R. Kotamraju, B. Ranscht, S. Krajewski, T. Teesalu, S. Bhatia, M. J. Sailor and E. Ruoslahti, *Nat. Commun.* 2016, **7**, 11980.

(80) A. S. Woods and S. Ferre, *J. Proteom. Res.* 2005, **4**, 1397.

(81) S. N. Jackson, S. C. Moyer and A. S. Woods, *J. Am. Soc. Mass Spectrom.* 2008, **19**, 1535.

(82) U. K. Shigdel, J. Zhang and C. He, *Angew. Chem. Int. Ed.* 2008, **47**, 90.

(83) S. G. F. Rasmussen, H.-J. Choi, D. M. Rosenbaum, T. S. Kobilka, F. S.; Thian, P. C. Edwards, M. Burghammer, V. R. P. Ratnala, R. Sanishvili, R. F. Fischetti, G. F. X. Schertler, W. I. Weis and B. K. Kobilka, B. K. *Nature* 2007, **450**, 383.

(84) V. Cherezov, D. M. Rosenbaum, M. A. Hanson, S. G. F. Rasmussen, F. S. Thian, T. S.; Kobilka, H.-J. Choi, P. Kuhn, W. I. Weis, B. K. Kobilka and R. C. Stevens, *Science* 2007, **318**, 1258.

(85) T. Sekiguchi, M. Tamura, H. Oba, P. Carçarbal, R. R. Lozada-Garcia, A. Zehnacker-Rentien, G. Gregoire, S. Ishiuchi and M. Fujii, *Angew. Chem,. Int. Ed.* 2018, **57**, 5626.

(86) A. M. Ring, A. Manglik, A. C. Kruse, M. D. Enos, W. I. Weis, K. C. Garcia and B. K. Kobilka, *Nature* 2013, **502**, 575.

(87) J. T. Sharp, Nitrile Ylides and Nitrile Imines. in the Chemistry of Heterocyclic Compounds 59: *Synthetic Applications of 1,3-Dipolar Cycloaddition Chemistry Toward Heterocycles and NaturalProducts*; Padwa, A., Pearson, W. H., Eds.; John Wiley & Sons: NewYork, 2002.

(88) W. Song, Y. Wang, J. Qu, M. M. Madden, Q. Lin, A Photoinducible 1,3-Dipolar Cycloaddition Reaction for Rapid, Selective Modification of Tetrazole-Containing Proteins. *Angew. Chem. Int Ed. Engl.* 2008, **47**, 2832.

(89) A. S. Shawali, Reactions of Heterocyclic Compounds with Nitrilimines and Their Precursors. *Chem. Rev.* 1993, **93**, 2731.

(90) D. L. Marshall, J. P. Menzel, B. I. McKinnon, J. P. Blinco, A. J. Trevitt, C. Barner-Kowolik and S. J. Blanksby, *Anal. Chem.* 2021, **93**, 8091.

(91) C. Bleiholder, S. Osbum, T. D. Williams, S. Suhai, M. Van Stipdonk, A. G. Harrison, and B. Paizs, *J. Am. Chem. Soc*. 2008, **130**, 17774.

(92) J. Novák, K. Lemr, K. A. Schug and V. Havlíček, *J. Am. Soc. Mass Spectrom.* 2015, **26**, 1780.